

^{235}U – ^{231}Pa age dating of uranium materials for nuclear forensic investigation†

Cite this: *J. Anal. At. Spectrom.*, 2013, **28**, 666

Gary R. Eppich,^{*} Ross W. Williams, Amy M. Gaffney and Kerri C. Schorzman

Age dating of nuclear material can provide insight into source and suspected use in nuclear forensic investigations. We report here a method for the determination of the date of most recent chemical purification for uranium materials using the ^{235}U – ^{231}Pa chronometer. Protactinium is separated from uranium and neptunium matrices using anion exchange resin, followed by sorption of Pa to an SiO_2 medium. The concentration of ^{231}Pa is measured by isotope dilution mass spectrometry using ^{233}Pa spikes prepared from an aliquot of ^{237}Np and calibrated in-house using the rock standard Table Mountain Latite and the uranium isotopic standard U100. Combined uncertainties of age dates using this method are 1.5 to 3.5 %, an improvement over alpha spectrometry measurement methods. Model ages of five uranium standard reference materials are presented; all standards have concordant ^{235}U – ^{231}Pa and ^{234}U – ^{230}Th model ages.

Received 7th February 2013

Accepted 14th March 2013

DOI: 10.1039/c3ja50041a

www.rsc.org/jaas

Introduction

The illicit trafficking of uranium presents a significant threat to the safety and security of the world. Nuclear forensic analyses, alongside conventional forensics, can provide valuable insight into the source, destination, and suspected use of interdicted nuclear materials. In this context, the age of a uranium-rich sample, defined as the time since the most recent chemical purification, is a useful descriptive parameter of the material that does not require comparison against a database. The ^{235}U – ^{231}Pa chronometer, commonly used in geochemistry (*e.g.*, ref. 1 and 2), is particularly amenable to age determination of uranium-rich materials due to high uranium concentration and, in some cases, ^{235}U -enriched isotopic composition. It must be kept in mind that the “age” is really a “model-age”, because it depends on the model assumptions, first, of closed-system behavior (no loss of ^{231}Pa , or gain other than from decay of ^{235}U), and second, that the initial concentration of ^{231}Pa at the time of U purification was zero. However, in this paper, we dispense with the prefix “model” when using the terms “age” and “date”, but it is implicit. The ^{235}U – ^{231}Pa chronometer can be used in concert with the ^{234}U – ^{230}Th chronometer (*e.g.*, ref. 3–5) to assess the accuracy of the age. In the case of concordant ages using two different chronometers, confidence in that age as the purification date of U is strengthened. If the ages are discordant, one, or both, may be inaccurate, or the sample may have experienced a complex, multi-stage purification process

affecting the daughter isotopes differently. In this case, the younger age represents the maximum possible age of the material, a useful datum in a nuclear forensic study.

In this paper, we present the first open-literature mass spectrometry study of the ^{235}U – ^{231}Pa chronometer for nuclear forensic investigations. Uranium-rich materials were analyzed for ^{235}U and ^{231}Pa concentrations by multi-collector inductively coupled plasma mass spectrometry (MC-ICPMS). Dates for a suite of certified reference materials distributed by New Brunswick Laboratory (NBL CRMs, uranium isotopic composition varying from depleted to highly enriched) are presented. Chemical separation techniques used in this study have been optimized for uranium matrices, resulting in simplified procedures and improved Pa recovery. Calibration of the ^{233}Pa spike, using both the rock-standard Table Mountain Latite (TML)^{6,7} and NBL CRM U100, is described, as are the age calculations, including a thorough treatment of uncertainty.

Dates using the ^{235}U – ^{231}Pa chronometer show excellent agreement with ^{234}U – ^{230}Th dates⁵ for all of the NBL CRMs analyzed in this study. Expanded uncertainties on ^{235}U – ^{231}Pa ages are 1.5–3.5%, an improvement over the 3.5–5% uncertainties reported by alpha spectrometry for the ^{235}U – ^{231}Pa chronometer.⁸ In all but one case (NBL CRM U100), dates are older than reported production dates, suggesting incomplete purification of U from the daughters ^{230}Th and ^{231}Pa during the production of these standards.

Methods

Production and calibration of the ^{233}Pa spike

Determination of the ^{235}U – ^{231}Pa age depends on precise and accurate measurement of ^{235}U and ^{231}Pa concentration.

Lawrence Livermore National Laboratory, Chemical Sciences Division, 7000 East Avenue, Livermore, California, USA. E-mail: eppich1@llnl.gov

† Electronic supplementary information (ESI) available. See DOI: 10.1039/c3ja50041a

Measurement of ^{235}U concentration by isotope dilution mass spectrometry (IDMS) is a routine procedure in geochemistry and nuclear forensics, and is described elsewhere (e.g., ref. 5). Measurement of ^{231}Pa concentration can be performed by IDMS with ^{233}Pa as the spike isotope. Due to the short half-life of ^{233}Pa (26.967 ± 0.004 days⁹), no certified ^{233}Pa spike exists. Rather, the spike must be prepared immediately prior to use and calibrated for ^{233}Pa concentration (atoms of $^{233}\text{Pa} \text{ g}^{-1}$) for its working-lifetime of approximately 3–4 months.

In this study, ^{233}Pa spikes were prepared from a ^{237}Np ($t_{1/2} = 2.14$ My, alpha decay to ^{233}Pa) starting material (Fig. 1, panel A). Approximately 20 mg of ^{237}Np with ^{233}Pa in secular equilibrium was dissolved in 9 M HCl + 0.05 M HF in a Teflon vial with 0.1 mL of concentrated HClO_4 . The Np was dried and re-dissolved in ~ 6 mL of 9 M HCl + 25 μL saturated H_3BO_3 + 50 μL concentrated HNO_3 . A Poly-Prep column (Bio-Rad) was loaded with 4 mL AG-1 X8 (100–200 mesh) anion exchange resin (Bio-Rad) and conditioned with >12 mL 9 M HCl. The Np solution was loaded on the column and the vial was rinsed twice with 1 mL 9 M HCl, and the rinses were loaded onto the column. The column was then washed with 4 mL 9 M HCl. Some Np (as Np(v)) is not sorbed on the resin and is recovered in the load and rinses. At this point, sorbed Np was clearly visible as a dark band in the top 1–2 mL of the resin bed. A new Teflon vial was then placed underneath the column to collect the Pa fraction, which was eluted with 12 mL 9 M HCl + 0.01 M HF (added in

2 mL increments). Throughout this procedure, care was taken to avoid disturbing the resin, ensuring that sorbed Np remained in the upper 2 mL of the resin bed. Several drops of concentrated HClO_4 were added to the vial containing the Pa, and the solution was dried. A Teflon vial was then positioned underneath the column to recover Np, which was eluted with 30–60 mL 1 M HCl + 0.5 M HF, combined with the load and rinse fraction, dried and stored for future production of ^{233}Pa spikes. The Pa fraction was re-dissolved in 9 M HCl + 25 μL of saturated H_3BO_3 + 50 μL of concentrated HNO_3 , and the anion exchange separation technique was repeated using a smaller column volume (~ 2 mL) and proportionally smaller load, wash, and elution volumes.

Following the two previous anion exchange separation steps, the Pa fraction was dried and re-dissolved in 2% HNO_3 (by volume) + 25 μL of saturated H_3BO_3 . The next purification steps take advantage of the well-known behavior of Pa to sorb to SiO_2 media. Quartz wool serves as the separation medium and is packed in a Poly-Prep column to a volume of approximately 2 mL and conditioned with >6 mL of 2% HNO_3 . The hydrolyzed species Pa(OH)_5 readily sorbs to the wool, and other elements such as Np and U wash through. Pa is recovered by adding trace HF to the elution solution.

The Pa solution was loaded onto the column. The vial was rinsed with 3 mL of 2% HNO_3 , and the rinses were added to the column. The column was washed with 4 mL 2% HNO_3 . A new

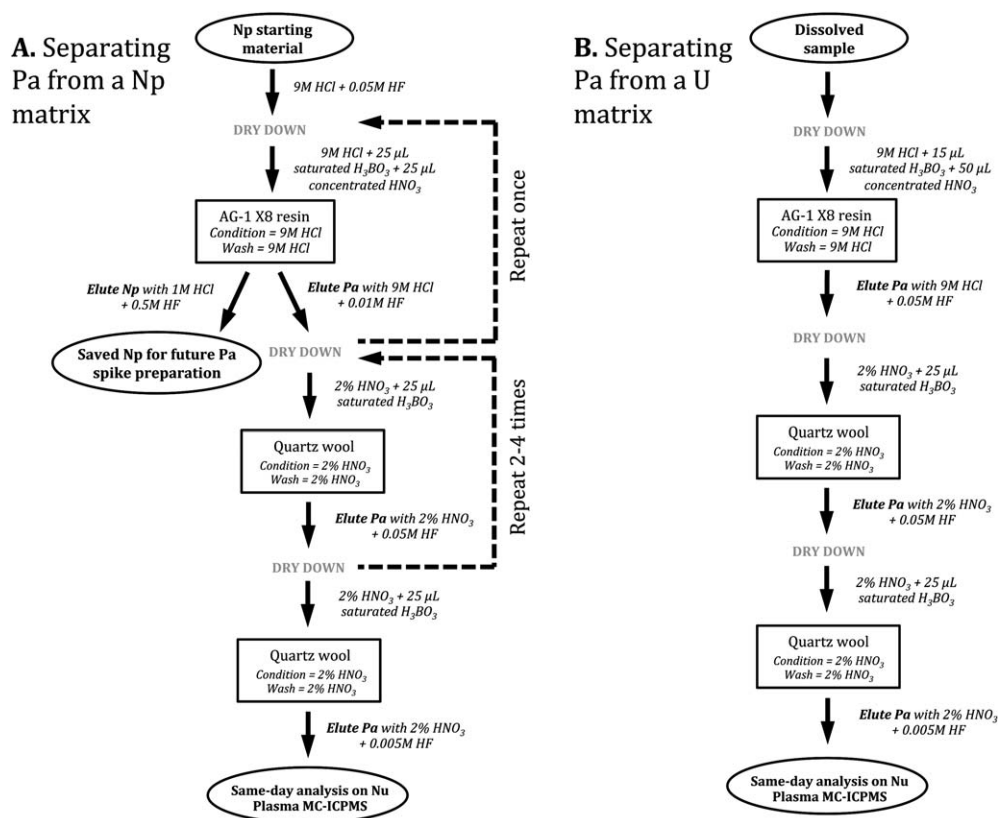


Fig. 1 Schematic diagram of procedures used to separate protactinium from a Np matrix (panel A) and a U matrix (panel B). Concentrated HClO_4 should be added to each sample immediately prior to each dry down step. See text for additional details.

Teflon vial was then placed under the column to collect Pa which was eluted with 6 mL 2% HNO₃ + 0.05 M HF, added in increments of 2 mL. Several drops of concentrated HClO₄ were added to the vial containing Pa, and it was dried and re-dissolved in 2% HNO₃. The quartz wool separation technique was repeated at least two more times in order to achieve the maximum possible separation of Pa from Np. The Np/Pa of the spike was assessed after each column by analyzing a dilute fraction of the solution with a Nu Plasma MC-ICPMS at Lawrence Livermore National Laboratory (LLNL). A 5–10 μL aliquot of the spike was diluted ~1000×, and the solution was screened by measuring the signal intensity of ²³⁷Np and ²³³Pa on the ion-counting electron multipliers. Purification of Pa was considered adequate when the signal intensity of ²³⁷Np was an order of magnitude lower than the signal intensity of ²³³Pa. Production of ²³³Pa from the alpha decay of ²³⁷Np is negligible for ²³⁷Np/²³³Pa < 0.1, which represents a Pa/Np separation factor of approximately 10¹⁰. At the same time, the amount of ²³³Pa available was estimated from the screening dilution and the instrument sensitivity factors, and the final spike solutions were prepared in an appropriate volume of 1 M HNO₃ + 0.05 M HF so that ²³³Pa would be approximately 1.5 to 3 × 10¹⁰ atoms per g spike.

Three ²³³Pa spikes were prepared for this study (Table 1). Calibration of each ²³³Pa spike was performed by IDMS using ²³¹Pa as the tracer isotope. Because no certified reference material for ²³¹Pa concentration exists, we used the rock standard Table Mountain Latite (TML), which is generally agreed to have the natural radioactive decay-series in secular equilibrium⁶ and has been used by the geochemistry community for ²³³Pa tracer calibration (e.g., ref. 1 and 10). The concentration of ²³¹Pa (atoms ²³¹Pa g⁻¹ TML) can be calculated by measuring the ²³⁵U concentration by IDMS and using eqn (1),

$$n_{231} = \frac{n_{235}\lambda_{235}}{\lambda_{231}} \quad (1)$$

where n_{235} and n_{231} are atoms of ²³⁵U g⁻¹ TML and atoms of ²³¹Pa g⁻¹ TML, and λ_{235} and λ_{231} are the decay constants of ²³⁵U and ²³¹Pa, respectively. Data used for the calculation of spike ²³³Pa concentration following this method are presented in ESI, Table S1.† However, well-known difficulties involved in the separation of Pa from silicate matrices (e.g., ref. 11 and 12) were observed here as well. After dissolution of TML by standard methods using HF there may have been Al- and Na-bearing fluoride compounds in solution that are highly compatible with Pa and notoriously difficult to dissolve. Low Pa recovery was observed in some TML calibration samples. We interpret this as incomplete destruction of such compounds which prevents Pa from behaving predictably in acidic ionic solution. Approximately half of the attempted TML calibration samples failed, and only the results for those analyses with Pa recoveries greater than ~10% are listed in Table 1.

Spike calibration was also performed using NBL CRM U100, a nominally 10% enriched (10.190 ± 0.010 atom% ²³⁵U) uranium isotopic reference material with a reported purification date of 8-Jan-1959.⁵ Williams and Gaffney⁵ used the ²³⁴U–²³⁰Th chronometer on duplicate solutions of U100 to

obtain dates of 16-Feb-1959 ± 88 days and 6-Mar-1959 ± 91 days. Uncertainties on the ²³⁴U–²³⁰Th dates overlap with the reported date of purification. These results demonstrate that chemical purification of ²³⁴U from the daughter nuclide ²³⁰Th was complete (negligible initial ²³⁰Th on the date of most recent purification). Until a certified ²³¹Pa tracer is available, and if the ²³¹Pa concentration on the purification date is also negligible, U100 is an ideal material to use for ²³³Pa spike calibration, avoiding the difficulties observed in separating Pa from the silicate matrix of TML. The atomic ratio of ²³¹Pa/²³⁵U can be calculated for any given time using eqn (2),

$$\frac{n_{231}}{n_{235}} = \frac{\lambda_{235}}{\lambda_{231} - \lambda_{235}} (1 - e^{(\lambda_{235} - \lambda_{231})t}) \quad (2)$$

where n_{231} is the number of atoms of ²³¹Pa g⁻¹ U100, n_{235} is the number of atoms of ²³⁵U g⁻¹ U100, t is the time elapsed since purification (8-Jan-1959), λ_{235} is the decay constant of ²³⁵U, and λ_{231} is the decay constant of ²³¹Pa. Data used for the calculation of the ²³³Pa concentration of the three spikes used in this study are presented in ESI, Table S2.† Calibration of the ²³³Pa tracer using TML and U100 should produce the same result, if the initial ²³¹Pa in U100 is negligible. The results presented here indicate that it is negligible, and is addressed in detail below.

To calibrate the ²³³Pa tracer, aliquots of TML and U100 containing between 5 × 10⁸ and 1 × 10¹⁰ atoms of ²³¹Pa were transferred to Teflon beakers. An aliquot of the spike containing approximately the same number of atoms of ²³³Pa was added (typically 0.25–3 g of ²³³Pa spike). The mixture was equilibrated by heating, sealed, on a hot plate for several hours. After equilibration, ~50 μL concentrated HClO₄ was added to each mixture. Chemical separation of Pa was similar to the procedure used for separating Pa from Np, with a few modifications (Fig. 1, panel B). After the mixtures were dried down, they were re-dissolved in 1 mL 9 M HCl + 50 μL concentrated HNO₃ + 15 μL saturated H₃BO₃. A ~2 mL resin bed of AG-1 X8 (100–200 mesh) was prepared in Poly-Prep columns, and the resin was conditioned with >6 mL 9 M HCl. Samples were loaded on columns, and the vials and columns were washed with 9 M HCl to remove matrix elements while Pa remained sorbed on the resin. New Teflon vials were then placed underneath the columns, and Pa was eluted using 6 mL of 9 M HCl + 0.05 M HF. A few drops of concentrated HClO₄ were added to each Pa fraction before being dried. Samples were then brought up 1 mL 2% HNO₃ + 25 μL saturated H₃BO₃ for Pa separation using the quartz wool technique discussed above. The quartz wool Pa separation was performed twice, with the Pa fractions dried after the addition of 3–5 drops HClO₄ between the separations. For the second quartz wool step, 3 mL 2% HNO₃ + 0.005 M HF was used to elute Pa. Samples were not dried down at this point. Instead, this solution was analyzed directly on the day of final separation to minimize in-growth of ²³³U from the beta-decay of ²³³Pa.

Measurement of ²³¹Pa/²³³Pa was performed using a Nu Plasma MC-ICPMS at LLNL. Pa was measured using a static simultaneous pulse-counting routine (40 cycles, 10 seconds integration time per cycle). Signal intensities on ²³¹Pa and ²³³Pa were typically on the order of 10³ to 10⁴ cps for all analyses

Table 1 ^{233}Pa spike calibration data. See ESI† for calculation of ^{233}Pa g^{-1} spike by isotope dilution. Data in bold represent the calibration point used to construct the calibration curve for each spike. Data used to calculate measured atoms ^{233}Pa g^{-1} spike is explained in the text, using data from ESI, Table S1† (U100) and ESI, Table S2† (TML). Calculation of the calibration curve atoms ^{233}Pa g^{-1} spike is explained in the text, using the decay constant $\lambda^{233}\text{Pa} = 2.5704 \times 10^{-2}$ (ref. 9)

Sample	Analysis date/ time	Measured atoms ^{233}Pa g^{-1} spike	Standard uncertainty	% Uncert.	Calibration curve atoms ^{233}Pa g^{-1} spike	Standard uncertainty	Difference (calibration curve – measured)	% Difference
Pa spike-1								
TML (3)	8/4/11 19:26	2.808×10^{10}	2.1×10^8	0.76	2.766×10^{10}	2.6×10^8	4.200×10^8	1.52
TML (5)	8/18/11 18:27	1.932×10^{10}	1.8×10^8	0.93	1.932×10^{10}	1.8×10^8	—	—
U100 #2 (1)	8/15/11 20:04	2.081×10^{10}	1.2×10^8	0.58	2.083×10^{10}	1.9×10^8	-2.580×10^7	-0.12
U100 #2 (2)	12/1/11 17:44	1.330×10^9	1.3×10^7	0.97	1.301×10^9	1.2×10^7	2.870×10^7	2.21
Pa spike-2								
U100 #2 (1)	1/31/12 15:40	2.081×10^{10}	1.0×10^8	0.49	2.081×10^{10}	1.0×10^8	—	—
U100 #2 (2)	1/31/12 16:06	2.079×10^{10}	1.0×10^8	0.50	2.080×10^{10}	1.0×10^8	-9.481×10^6	-0.05
U100 #2 (3)	1/31/12 16:32	2.076×10^{10}	1.1×10^8	0.52	2.079×10^{10}	1.0×10^8	-3.844×10^7	-0.18
U100 #2 (4)	2/28/12 19:16	1.005×10^{10}	6.6×10^7	0.65	1.009×10^{10}	5.0×10^7	-4.550×10^7	-0.45
U100 #2 (5)	3/19/12 18:52	6.008×10^9	3.3×10^7	0.54	6.040×10^9	3.0×10^7	-3.172×10^7	-0.53
TML (4)	3/3/12 19:09	9.185×10^9	2.9×10^7	0.32	9.110×10^9	4.5×10^7	7.496×10^7	0.82
TML (5)	3/3/12 19:35	9.120×10^9	3.0×10^7	0.33	9.105×10^9	4.5×10^7	1.452×10^7	0.16
TML (6)	3/3/12 20:02	9.170×10^9	3.0×10^7	0.33	9.101×10^9	4.5×10^7	6.927×10^7	0.76
Pa spike-3								
U100 #2 (1)	6/18/12 17:49	1.527×10^{10}	1.6×10^8	1.04	1.527×10^{10}	1.6×10^8	—	—
U100 #2 (2)	6/18/12 18:15	1.534×10^{10}	1.6×10^8	1.04	1.526×10^{10}	1.6×10^8	7.659×10^7	0.50
U100 #2 (3)	8/30/12 20:03	2.311×10^9	2.1×10^7	0.91	2.333×10^9	2.4×10^7	-2.189×10^7	-0.94
U100 #2 (4)	9/19/12 15:42	1.401×10^9	1.6×10^7	1.12	1.402×10^9	1.5×10^7	-9.733×10^5	-0.07

except low-recovery TML analyses. Masses 235 and 232 were monitored on Faraday detectors to address the completeness of Pa separation from matrix elements (potential tailing of ^{235}U or ^{232}Th -hydride at mass 233). The signal intensities of acid blanks, measured before each analysis, were typically <1 cps. Corrections for instrumental mass bias and detector cross-calibration factors were determined by measuring the uranium isotopic standard U010.

The spike concentration (atoms ^{233}Pa g^{-1} spike) is calculated using eqn (3),

$$n_{233} = \frac{n_{231}m_{\text{std}}}{m_{\text{spike}}R} \quad (3)$$

where n_{233} is the number of atoms of ^{233}Pa g^{-1} spike, n_{231} is the calculated number of atoms of ^{231}Pa g^{-1} TML (eqn (1)) or U100 solution (eqn (2)), R is the measured $^{231}\text{Pa}/^{233}\text{Pa}$ ratio, and m_{std} and m_{spike} are the masses (in grams) of the standard solution and spike solution used for the calibration sample, respectively. See ESI, Tables S1 and S2† for the data used to calculate ^{233}Pa concentration.

The ^{233}Pa spike calibration curve is a mathematical model of the decay of ^{233}Pa over time. The curve is calculated for any time t (relative to the time of initial calibration) using eqn (4),

$$N_{233t} = N_{233C}e^{(-\lambda_{233}t)} \quad (4)$$

where N_{233t} is the number of atoms of ^{233}Pa g^{-1} spike at time t , N_{233C} is the measured number of atoms of ^{233}Pa g^{-1} spike at the time of calibration (result of eqn (3)), and λ_{233} is the decay constant of ^{233}Pa . Calibration checks are measured throughout the working-life of each spike (about 3–4 months) in order to assess the accuracy of the calibration over time. Calibration curves and calibration points are shown in panels A, C, and E of Fig. 2. The uncertainty envelope of each calibration curve, and the position of each calibration point with respect to the calibration curve, is shown in panels B, D, and F of Fig. 2.

The ^{233}Pa spikes, Pa spike-1 and Pa spike-2, were calibrated using both TML and U100 (Fig. 2, panels A–D). The Pa spike-1 calibration curve was constructed using TML and the Pa

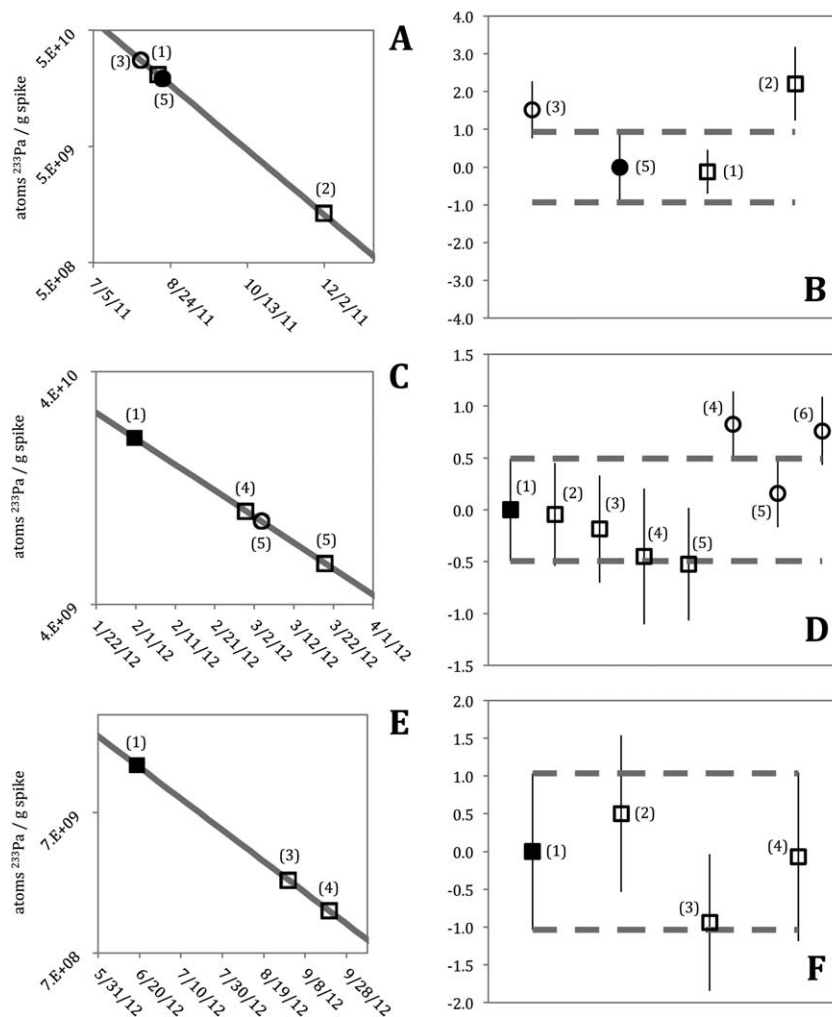


Fig. 2 Calibration curves and calibration points for Pa spike-1 (panels A and B), Pa spike-2 (panels C and D), and Pa spike-3 (panels E and F). See Table 1 for calibration point data. Squares, U100 calibration points; circles, TML calibration points; data labels, analysis identification number (see Table 1). In panels A, C, and E, the solid gray line is the calibration curve (calculated using eqn (4)), which represents the decay of ²³³Pa in each spike over time. The y-axis scales in panels A, C, and E are logarithmic. Closed symbols represent the calibration point upon which the calibration curve is built. In panels B, D, and F, the dotted gray lines represent the uncertainty envelope of the calibration curve. The y-axis scales of panels B, D, and F represent the % difference from the number of atoms of ²³³Pa g⁻¹ spike as defined by the black calibration points. Uncertainty bars in panels A, C, and E are smaller than the symbols.

spike-2 calibration curve was constructed using U100. The accuracy of each curve was assessed throughout the working life of the spike using replicate measurements of TML and U100. If the assumption of negligible initial ²³¹Pa underlying eqn (2), and the assumption of secular equilibrium underlying eqn (1), are accurate, then the measured atoms ²³³Pa g⁻¹ spike for each replicate analysis of TML and U100 should fall within the uncertainty envelope for a given calibration curve, regardless of which standard is used to calibrate the ²³³Pa spike.

The measurement TML (5) was used to construct the Pa spike-1 calibration curve, and the measurements TML (3), U100 #2 (1), and U100 #2 (2) were used as calibration checks (Fig. 2, panels A and B). Excellent agreement between TML and U100 is observed for two of the three calibration points: TML (3) and U100 #2 (1) fall within the uncertainty envelope of the calibration curve. Note that U100 #2 (2) falls slightly outside of the

uncertainty envelope of the Pa spike-1 calibration curve. This analysis was performed towards the end of the working life of the spike (~4 months after production), and most of the ²³³Pa had decayed away by that point. It is also possible that evaporation of the spike over time may have contributed to the slightly higher ²³³Pa concentration as determined by U100 #2 (2).

The measurement U100 #2 (1) was used to construct the Pa spike-2 calibration curve, and three TML calibration points and four additional U100 calibration points were used as calibration checks (Fig. 2, Panels C and D). Points U100 #2 (2) and U100 #2 (3) were analyzed in the same analytical run as U100 #2 (1); these three points show excellent agreement. U100 #2 (4) and U100 #2 (5) were analyzed approximately 1 and 2 months after calibration, respectively. These two calibration points also fall within the uncertainty envelope of the calibration curve. Poor recovery of Pa from the TML silicate matrix during chemical

separation may explain the slight deviation of TML (4) and TML (6) from the calibration curve. TML (5) shows excellent agreement with the U100 calibration curve.

Having established that TML and U100 calibrations produce similar calibration curves, Pa spike-3 was calibrated using only replicate measurements of U100. The measurement of U100 #2 (1) was used to construct the calibration curve, and three replicate measurements of U100 were used as calibration checks. Excellent agreement between all calibration points is observed, even for analyses performed 3–4 months after tracer production.

Isotope dilution measurement of uranium reference standards

Concentrations of ^{235}U and ^{231}Pa were measured by IDMS in uranium reference standards U005-A, U030-A, U100, U630, and 125-A. In the case of U100, a separate digestion of the starting material (U100 #1) was used. Solutions U005-A, U030-A, and U100 were the same solutions analyzed using the ^{234}U – ^{230}Th chronometer by ref. 5. Two new digestions each of U630 and 125-A were prepared. The ^{234}U – ^{230}Th ages of these materials were determined and are reported here for the first time (Table 3). Measurements of ^{235}U concentration were made by IDMS with a ^{233}Pa spike following the analytical routines described by ref. 5. Analyses were performed on a Nu Plasma MC-ICPMS using a static routine with ^{235}U and ^{233}U measured on Faraday detectors. Correction for instrumental mass bias was made using the uranium isotopic standard U010.

^{231}Pa was measured by IDMS in these samples using the procedures and ^{233}Pa spikes described above. The sample concentration of ^{231}Pa is calculated for the time of analysis using eqn (5),

$$n_{231} = \frac{R m_{\text{spike}} n_{233}^0 e^{(-\lambda_{233} t)}}{m_{\text{sample}}} \quad (5)$$

where n_{231} is the number of atoms of ^{231}Pa g^{-1} sample, R is the $^{231}\text{Pa}/^{233}\text{Pa}$ measured ratio, m_{spike} is the spike mass in grams, n_{233}^0 is the number of atoms of ^{233}Pa g^{-1} spike on the date of calibration, λ_{233} is the decay constant of ^{233}Pa , t is the number of days between initial spike calibration and analysis, and m_{sample} is the sample mass in grams. Data used for this calculation are presented in ESI, Table S3†. Procedural blanks were also prepared and measured with each analysis batch using the same spiking and chemical separation procedures as for the samples. Signal intensities for the blanks at ^{231}Pa were negligible at <1 cps, and no procedural blank corrections were made.

Ages are calculated using eqn (6),

$$t = \left(\frac{1}{\lambda_{235} - \lambda_{231}} \right) \ln \left(1 + \frac{R(\lambda_{235} - \lambda_{231})}{\lambda_{235}} \right) \quad (6)$$

where t is the ^{235}U – ^{231}Pa age, λ_{235} is the decay constant of ^{235}U , λ_{231} is the decay constant of ^{231}Pa , and R is the $^{231}\text{Pa}/^{235}\text{U}$ ratio. All uncertainty calculations in this study follow the guidelines of JCGM 100:2008. An uncertainty budget for the ^{235}U – ^{231}Pa age of

Table 2 Representative uncertainty budget

	Contribution to combined uncertainty (%)
U100 #1 Model age	
Model age	
$\lambda^{235}\text{U}$	0.69
$\lambda^{231}\text{Pa}$	<0.01
$^{231}\text{Pa}/^{235}\text{U}$	
Atoms ^{235}U g^{-1} sample	1.01
Atoms ^{231}Pa g^{-1} sample	
$^{231}\text{Pa}/^{233}\text{Pa}$	62.82
Spike weight	<0.01
Sample weight	<0.01
Days since initial ^{233}Pa spike calibration	<0.01
$\lambda^{233}\text{Pa}$	0.02
Atoms ^{233}Pa g^{-1} spike	
Standard aliquot weight	<0.01
Spike weight	<0.01
$^{231}\text{Pa}/^{233}\text{Pa}$	30.25
Atoms ^{231}Pa g^{-1} standard	
$\lambda^{235}\text{U}$	5.20
$\lambda^{231}\text{Pa}$	<0.01
Time	<0.01
Total	100.00

U100 #1 is presented in Table 2. The sources of uncertainty in the ^{235}U – ^{231}Pa age, in order of decreasing importance, are:

- (1) $^{231}\text{Pa}/^{233}\text{Pa}$ measurement of the sample;
- (2) $^{231}\text{Pa}/^{233}\text{Pa}$ measurement for spike calibration;
- (3) the decay constant of ^{235}U in the calculation of atoms ^{231}Pa g^{-1} U100 standard for the spike calibration (eqn (2));
- (4) isotope dilution measurement of atoms of ^{235}U g^{-1} sample;
- (5) the decay constant of ^{235}U in the calculation of the age (eqn (6)); and
- (6) the decay constant of ^{233}Pa used in the calculation of sample ^{231}Pa concentration (eqn (5)).

The uncertainties from weighing and the decay constant of ^{231}Pa contribute <0.01%. As the largest component of the uncertainty on the age is related to the measurement of $^{231}\text{Pa}/^{233}\text{Pa}$, efforts to improve this technique should focus on this. However, the low concentration of ^{231}Pa in uranium-rich materials produced in the nuclear age presents an intrinsic challenge. In addition, efforts to improve ratio measurements would do nothing to improve upon the inherent uncertainty posed by the initial presence of ^{231}Pa in the case of incompletely purified samples.

Results

Ages for U100 (solution #1) and four additional NBL CRMs are presented in Table 3. Measurement of U100 #1 resulted in a ^{235}U – ^{231}Pa date of 2-Oct-1958 \pm 321 days. This date overlaps within uncertainty of the ^{234}U – ^{230}Th date of 16-Feb-1959 \pm 88 days, measured on the same solution by ref. 5. That both

Table 3 Model ages of NBL CRMs

Sample ID	Reference date	Atoms ^{231}Pa g^{-1} sample	Standard uncertainty	Atoms ^{235}U g^{-1} sample	Standard uncertainty	$^{231}\text{Pa}/^{235}\text{U}$	Standard uncertainty	^{235}U - ^{231}Pa model age	Expanded uncertainty (years, $k = 2$)	Model date
U005-A #1 (1)	30-Aug-12	6.596×10^8	9.0×10^6	2.078×10^{16}	1.7×10^{13}	3.174×10^{-8}	4.4×10^{-10}	32.243	0.887	3-Jun-80
U005-A #1 (2)	30-Aug-12	6.636×10^8	9.1×10^6	2.078×10^{16}	1.7×10^{13}	3.194×10^{-8}	4.4×10^{-10}	32.442	0.889	22-Mar-80
U005-A #2 (1)	30-Aug-12	5.374×10^8	7.5×10^6	1.687×10^{16}	1.4×10^{13}	3.186×10^{-8}	4.4×10^{-10}	32.358	0.902	21-Apr-80
U005-A #2 (2)	30-Aug-12	5.371×10^8	7.4×10^6	1.687×10^{16}	1.4×10^{13}	3.184×10^{-8}	4.4×10^{-10}	32.338	0.889	29-Apr-80
U030-A #1	28-Feb-12	4.089×10^8	3.6×10^6	1.303×10^{16}	9.6×10^{12}	3.140×10^{-8}	2.8×10^{-10}	31.889	0.567	9-Apr-80
U030-A #2	28-Feb-12	2.764×10^8	2.3×10^6	8.819×10^{15}	6.6×10^{12}	3.134×10^{-8}	2.6×10^{-10}	31.830	0.530	30-Apr-80
U100 #1	28-Feb-12	1.772×10^9	1.4×10^7	3.372×10^{16}	2.8×10^{13}	5.257×10^{-8}	4.3×10^{-10}	53.407	0.879	2-Oct-58
U630 #1 (1)	19-Mar-12	2.142×10^9	1.5×10^7	9.452×10^{16}	1.4×10^{14}	2.266×10^{-8}	1.6×10^{-10}	23.018	0.334	13-Mar-89
U630 #1 (2)	29-Jun-12	2.156×10^9	2.6×10^7	9.452×10^{16}	1.4×10^{14}	2.281×10^{-8}	2.8×10^{-10}	23.167	0.561	29-Apr-89
U630 #2 (1)	29-Jun-12	2.521×10^{10}	3.0×10^8	1.113×10^{18}	1.4×10^{15}	2.265×10^{-8}	2.7×10^{-10}	23.004	0.554	27-Jun-89
125 A #1 (1)	19-Mar-12	1.010×10^{10}	7.1×10^7	5.772×10^{17}	7.7×10^{14}	1.750×10^{-8}	1.3×10^{-10}	17.773	0.257	11-Jun-94
125 A #1 (2)	28-Jun-12	1.033×10^{10}	1.7×10^8	5.772×10^{17}	7.7×10^{14}	1.790×10^{-8}	2.9×10^{-10}	18.175	0.598	26-Apr-94
125 A #2 (1)	19-Mar-12	1.381×10^{10}	9.7×10^7	7.886×10^{17}	1.0×10^{15}	1.751×10^{-8}	1.2×10^{-10}	17.782	0.255	7-Jun-94
125 A #2 (2)	28-Jun-12	1.412×10^{10}	2.3×10^8	7.886×10^{17}	1.0×10^{15}	1.791×10^{-8}	2.9×10^{-10}	18.190	0.599	20-Apr-94

Sample ID	Reference date	Atoms ^{230}Th g^{-1} sample	Standard uncertainty	Atoms ^{234}U g^{-1} sample	Standard uncertainty	$^{230}\text{Th}/^{234}\text{U}$	Standard uncertainty	^{234}U - ^{230}Th model age	Expanded uncertainty (years, $k = 2$)	Model date
U630 #1 (1)	19-Mar-12	6.098×10^{10}	2.1×10^8	9.232×10^{14}	1.5×10^{12}	6.605×10^{-5}	2.5×10^{-7}	23.372	0.184	3-Nov-88
U630 #1 (2)	19-Mar-12	6.098×10^{10}	2.1×10^8	9.232×10^{14}	1.5×10^{12}	6.605×10^{-5}	2.5×10^{-7}	23.372	0.184	3-Nov-88
U630 #2 (1)	29-May-12	7.201×10^{11}	1.8×10^9	1.087×10^{16}	1.6×10^{13}	6.623×10^{-5}	1.9×10^{-7}	23.434	0.142	21-Dec-88
125 A #1 (1)	19-Mar-12	2.729×10^{11}	9.4×10^8	5.321×10^{15}	4.3×10^{13}	5.129×10^{-5}	4.5×10^{-7}	18.147	0.321	25-Jan-94
125 A #1 (2)	19-Mar-12	2.729×10^{11}	9.4×10^8	5.321×10^{15}	4.3×10^{13}	5.129×10^{-5}	4.5×10^{-7}	18.147	0.321	25-Jan-94
125 A #2 (1)	19-Mar-12	3.728×10^{11}	1.3×10^9	7.269×10^{15}	5.9×10^{13}	5.128×10^{-5}	4.5×10^{-7}	18.146	0.321	25-Jan-94
125 A #2 (2)	19-Mar-12	3.728×10^{11}	1.3×10^9	7.269×10^{15}	5.9×10^{13}	5.128×10^{-5}	4.5×10^{-7}	18.146	0.321	25-Jan-94

systems are also in agreement with the purification date of 8-Jan-1959 adds confidence in the accuracy of these analyses, and that the assumptions intrinsic to the dating hold true for this sample.

Solutions of U005-A and U030-A were also the same as those analyzed by ref. 5. Two solutions of each standard were measured (#1 and #2; Table 3), and the two solutions of U005-A were each measured in duplicate. The average ^{235}U - ^{231}Pa dates of four U005-A analyses and two U030-A analyses are 26-Apr-1980 and 19-Apr-1980, respectively (results for individual

analyses are presented in Table 3 and Fig. 3). ^{235}U - ^{231}Pa dates for individual analyses overlap within uncertainty with the ^{234}U - ^{230}Th dates of ref. 5. However, both sets of dates are older than the reported purification dates. These results suggest that initial ^{230}Th and ^{231}Pa concentrations are non-negligible in these standards, resulting in older ages.

The ^{235}U - ^{231}Pa and ^{234}U - ^{230}Th dates of U630 and 125 A are presented in Table 3 and Fig. 3. These standards do not have reported purification dates and are currently in the process of being certified for ^{234}U - ^{230}Th age by New Brunswick Laboratory.

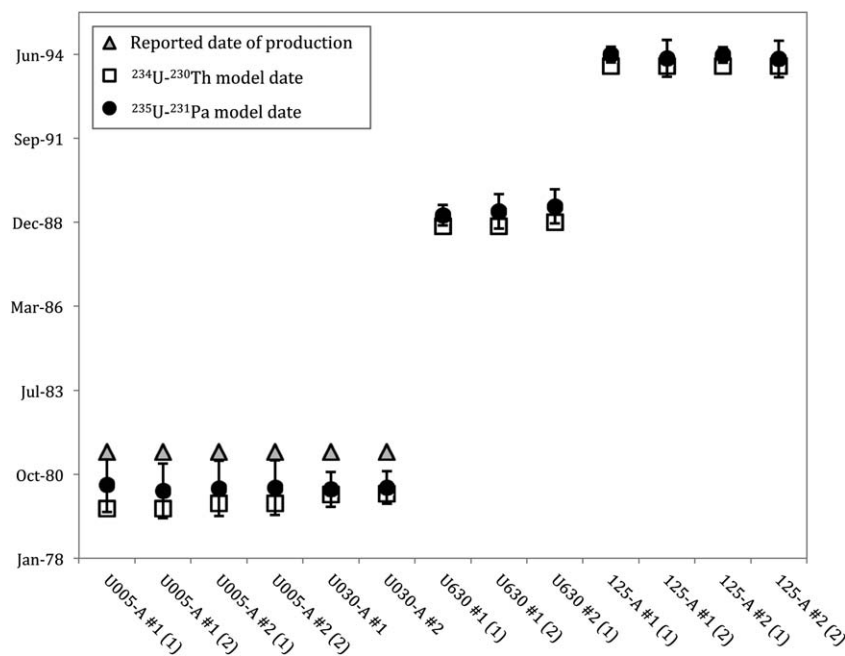


Fig. 3 Model ages of uranium standard reference materials. ^{234}U - ^{230}Th model ages for U005-A and U030-A are from ref. 5. Uncertainty bars for ^{234}U - ^{230}Th model ages are smaller than symbols.

Average ^{235}U - ^{231}Pa model dates of three U630 analyses (on solutions #1 and #2) and four 125 A (solutions #1 and #2) analyses are 28-Sep-1989 and 16-May-1994, respectively. Individual sample ages overlap within uncertainty with those determined for this study using the ^{234}U - ^{230}Th chronometer (27-Nov-1988 and 25-Jan-1994, respectively). In this case, the concordant dates indicate that the most recent chemical purification reduced Th and Pa to the same degree with respect to U. The assumption of age-dating, that both were reduced to zero at this time, cannot be proved.

In a nuclear forensic investigation, confidence that ages record the most recent chemical purification event is increased when more than one chronometer is used. The ^{235}U - ^{231}Pa chronometer can be used in concert with the more frequently utilized ^{234}U - ^{230}Th chronometer to assess age accuracy. Ages were concordant for both chronometers for all of the NBL CRMs measured in this study, but are not necessarily consistent with the known purification dates. These results suggest that the $^{230}\text{Th}/^{234}\text{U}$ and $^{231}\text{Pa}/^{235}\text{U}$ at the time of uranium purification were small but similar.

Acknowledgements

The authors would like to thank two anonymous reviewers who provided useful comments leading to an improved manuscript. Major support for this work was provided by the Office of Nonproliferation and International Security (NA-24), National Nuclear Security Administration, and the U.S. Department of Energy. This work was performed under the auspices of the U.S. Department of Energy by Lawrence Livermore National Laboratory under Contract DE-AC52-07NA27344. LLNL-JRNL-615952.

References

- 1 D. A. Pickett, M. T. Murrell and R. W. Williams, Determination of femtogram quantities of protactinium in geologic samples by thermal ionization mass spectrometry, *Anal. Chem.*, 1994, **66**, 1044–1049.
- 2 H. Cheng, R. L. Edwards, M. T. Murrell and T. M. Benjamin, Uranium–thorium–protactinium dating systematics, *Geochim. Cosmochim. Acta*, 1998, **62**, 3437–3452.
- 3 S. P. LaMont and G. Hall, Uranium age determination by measuring the $^{230}\text{Th}/^{234}\text{U}$ ratio, *J. Radioanal. Nucl. Chem.*, 2005, **264**, 423–427.
- 4 Z. Varga and G. Surányi, Production date determination of uranium-oxide materials by inductively coupled plasma mass spectrometry, *Anal. Chim. Acta*, 2007, **599**, 16–23.
- 5 R. W. Williams and A. M. Gaffney, ^{230}Th - ^{234}U model ages of some uranium standard reference materials, *Radiochim. Acta*, 2011, **1**, 31–35.
- 6 R. W. Williams, K. D. Collerson, J. B. Gill and C. Deniel, High Th/U ratios in subcontinental lithospheric mantle: mass spectrometric measurement of Th isotopes in Gaussberg lamproites, *Earth Planet. Sci. Lett.*, 1992, **111**, 257–268.
- 7 K. W. W. Sims, *et al.*, An inter-laboratory assessment of the thorium isotopic composition of synthetic and rock reference materials, *Geostand. Geoanal. Res.*, 2008, **32**(1), 65–91.
- 8 A. Morgenstern, C. Apostolidis and K. Mayer, Age determination of highly enriched uranium: separation and analysis of ^{231}Pa , *Anal. Chem.*, 2002, **74**, 5513–5516.
- 9 R. T. Jones, J. S. Merritt and A. Okazaki, A measurement of the thermal neutron capture cross-section of ^{232}Th , *Nucl. Sci. Eng.*, 1986, **93**, 171–180.

- 10 M. Regelous, S. P. Turner, T. R. Elliott, K. Rostami and C. J. Hawkesworth, Measurement of femtogram quantities of protactinium in silicate rock samples by multicollector inductively coupled plasma mass spectrometry, *Anal. Chem.*, 2004, **76**, 3584–3589.
- 11 K. A. Kraus and G. E. Moore, Anion-exchange studies. XV. Separation of protactinium and iron by anion-exchange in HCl–HF solutions, *J. Am. Chem. Soc.*, 1955, **77**, 1383–1384.
- 12 J. I. Kim, H. Lagally and H.-J. Born, Ion exchange in aqueous and in aqueous–organic solvents. Part I. Anion-exchange behavior of Zr, Nb, Ta and Pa in aqueous HCl–HF and in HCl–HF–organic solvent, *Anal. Chim. Acta*, 1973, **64**, 29–43.